Evaluating the structure and magnitude of the ash plume during the initial phase of the 2010 Eyjafjallajökull eruption using lidar observations and NAME simulations

H. F. Dacre, A. L. M. Grant, R. J. Hogan, S. E. Belcher,[1]

D. J. Thomson, B. J. Devenish, F. Marenco, M. C. Hort,[2] J. M. Haywood[23],

A. Ansmann, I. Mattis,[4]

L. Clarisse[5].

Abstract. The Eyjafjallajökull volcano in Iceland erupted explosively on 14 April 2010 emitting a plume of ash into the atmosphere. The ash was transported from Iceland towards Europe where mostly cloud-free skies allowed ground-based lidars at Chilbolton in England and Leipzig in Germany to estimate the mass concentration in the ash cloud as it passed overhead. The UK Met Office's Numerical Atmospheric-dispersion Modelling Environment, NAME, has been used to simulate the evolution of the ash cloud from the Eyjafjallajökull volcano during the initial phase of the ash emissions, 14-16 April 2010. NAME captures the timing and sloped structure of the ash layer observed over Leipzig, close to the central axis of the ash cloud. Relatively small errors in the ash cloud position, probably caused by the cumulative effect of errors in the driving meteorology en route, result in a timing error at distances far from the central axis of the ash cloud. Taking the timing error into account, NAME is able to capture the sloped ash layer over the UK.

Comparison of the lidar observations and NAME simulations has allowed an estimation of the plume height time-series to be made. It is necessary to include in the model input the large variations in plume height in order to accurately predict the ash cloud structure at long range. Quantitative comparison with the mass concentrations at Leipzig and Chilbolton suggest that around 3% of the total emitted mass is transported as far as these sites by small ($< 100\mu$m diameter) ash particles.

1. Introduction

On 14 April 2010 the character of eruption at Eyjafjallajökull volcano changed from basaltic lava fountaining to explosive emissions of high levels of ash, causing widespread disruption throughout Europe due to the closure of European airspace. Volcanic ash can cause significant problems for aircraft due to the reduction in visibility, abrasion of aircraft surfaces and even engine failure [*Casadevall*, 1994; *Guffanti et al.*, 2010]. Thus monitoring and forecasting the dispersion of ash clouds is important for human safety.

The responsibility for issuing advice to aviation about the geographic distribution of volcanic ash from volcanoes are provided by the Volcanic Ash Advisory Centres (VAAC's) with responsibility for different regions divided among different operational centres [*Witham et al.*, 2007]. The London VAAC is responsible for ash emitted from volcanoes in Iceland. The UK Met Office's dispersion model, NAME, is used operationally by the London VAAC to forecast the evolution of volcanic ash clouds. The NAME model uses driving meteorology from a numerical weather prediction (NWP) model and input of a number of parameters describing the volcanic source such as plume height, vertical distribution of ash and mass eruption rate [*Leadbetter and Hort*, 2011]. The aim of this paper is to compare NAME simulations of the initial phase of the ash emissions with ground-based lidar observations of ash layers over the UK and Germany with a view to understanding the dispersion of volcanic ash, estimating the plume height at the source and estimating the distal fine ash fraction which survives the near-source fall-out processes. Evaluation of NAME, using this natural point source release event, will also contribute to improvements in the methods used to simulate the transport and representation of volcanic ash in the model.

In this paper *plume height* is defined as the maximum height above mean sea level (amsl) that the ash plume reaches in the vicinity of the volcano vent. It is needed as an input to most volcanic ash dispersion models. *Particles* are defined as the entities dispersing in the atmosphere, which may be either unaggregated single grains of ash or aggregates, i.e. clusters of grains of ash. The *distal fine ash fraction* is defined as the fraction of the total emitted mass that is carried by small particles ($< 100\mu$m diameter) and transported long distances (of order 1000 km) from the volcano. Large particles, both single large grains and large aggregates, fall out close to the volcano. Aggregation can occur > 1000 km from the source, due to the interaction of

[1]Department of Meteorology, University of Reading, Earley Gate, PO Box 243, Reading, RG6 6BB, UK.

[2]Met Office, FitzRoy Road, Exeter EX1 3PB, UK.

[3]College of Engineering, Mathematics, and Physical Sciences, University of Exeter.

[4]Leibniz Institute for Tropospheric Research, Permoserstrasse 15, 04318 Leipzig, Germany.

[5]Spectroscopie de l'Atmosphère, Service de Chimie Quantique et Photophysique, Universitè Libre de Bruxelles, Brussels, Belgium

ash and ice particles which results in the formation of aggregates of ash-hydrometeors [*Durant et al.*, 2009; *Sparks et al.*, 1997] or due to electrostatic binding of aggregates [*James et al.*, 2002], but it is most effective near source. For models which don't represent aggregation processes the distal fine ash fraction is used as a scaling factor that is applied to the model concentrations to allow quantitative predictions of ash quantities at long-range.

In this paper the parameters describing the volcanic source are outlined in section 2. A description of the NAME dispersion model and simulations are given in section 3. The lidar observations at Chilbolton in southern England and Leipzig in Germany are described in section 1. A comparison of the lidar and NAME simulated ash cloud over Leipzig and Chilbolton for a constant plume height is given in section 5. Section 6 shows a similar comparison but for a varying plume height. Finally, discussion and conclusions are presented in section 7.

2. Parameters describing the effective volcanic source

Like many volcanic ash dispersion models, NAME does not represent the complex dynamics which occur close to the volcano and instead assumes an 'effective' source describing the injection of material into the atmosphere. The effective source is characterised by several key parameters.

2.1. Plume height

The height at which ash particles are emitted into the atmosphere at the source has a large influence on the vertical and horizontal structure of the ash plume downstream [*Webley et al.*, 2009]. This is due to the fact that wind speed and direction vary with height and can lead to layering of ash as observed in the radiosonde launch carried out from Stranraer on the 19 April 2010 by *Harrison et al.* [2010] and the lidar observations over Europe [*Marenco and Hogan*, 2010; *Ansmann et al.*, 2010; *Hogan et al.*, 2011]. In order to represent the evolution of the ash cloud accurately, it is necessary to accurately represent the height at which ash particles are emitted.

In this paper information about the Eyjafjallajökull eruption plume height is taken from measurements provided by the Icelandic Meteorological Office's C-band radar [*Petersen and Arason*, 2011]. There were time periods when no radar data were available. These periods occurred either because the radar cannot detect the plume when it is below 2.5 km, due to mountain ranges and the curvature of the Earth, or because the plume was obscured by water or ice clouds, or because the radar scan was missing. Furthermore, the maximum observed plume height may not be the maximum height at which ash is injected laterally into the atmosphere. However, for weak eruptions, such as Eyjafjallajökull, the difference is usually less than a few kilometers [*Mastin et al.*, 2009]. In this paper the sensitivity to plume height of the NAME volcanic ash predictions over the UK and Germany is investigated.

2.2. Vertical distribution of ash

Information on the lower boundary of the effective source is also difficult to ascertain. In general, by analogy with chimney plumes, one would expect most of the emitted ash from a large magnitude explosive eruption to be found well above the ground and close to the plume top (in the umbrella cloud) [*Sparks et al.*, 1997]. However, this may not be the case for long duration eruptions in which plume height is varying and interacting with the background atmosphere, for weak eruptions, or if the plume is collapsing to produce

pyroclastic density currents [*Mastin et al.*, 2009; *Bonadonna et al.*, 2002]. Because Eyjafjallajökull was a weak eruption, the minimum height for ash release used in this paper is set to the volcano summit height (1.6 km for Eyjafjallajökull) and ash is assumed to be emitted uniformly (in terms of mass mixing ratio) between the volcano summit and the maximum observed plume height. In an operational context this is a conservative choice which tries to avoid predicting no ash where a significant hazard may exist.

2.3. Mass Eruption Rate

At present there is no direct method of measuring the mass eruption rate of erupting volcanoes. As a result, many VAAC models, including NAME, use empirical relationships to relate observed maximum plume height to the eruption rate [*Wilson et al.*, 1978; *Sparks et al.*, 1997; *Mastin et al.*, 2009]. Details of the relationship used here and comparison with other relationships is included in the Appendix. In practice, for modelling long range transport, the important number to quantify is not the total mass eruption rate, but the fraction of total emitted mass present in the downstream ash cloud (i.e. carried by small ash particles which do not fall out close to the source). This distal fine ash fraction is used as a scaling factor that is applied to the model amounts to allow quantitative predictions of ash at long-range. *Mastin et al.* [2009] provided estimates of the fraction of emitted mass carried by small ash grains ($< 63\mu$m

Table 1. Ash particle size distribution used in NAME.

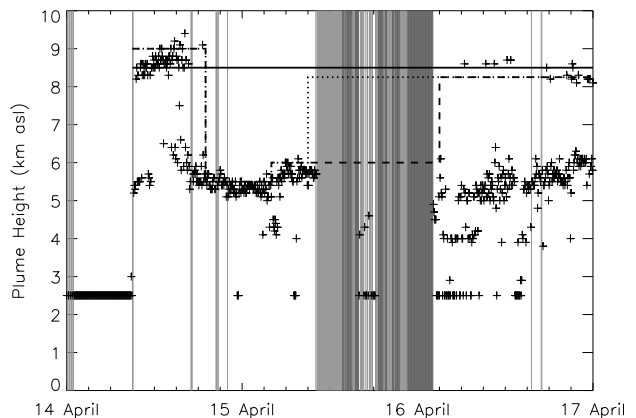| Particle diameter (μm)	Fraction of mass (%)
0.1-0.3	0.1
0.3-1.0	0.5
1.0-3.0	5.0
3.0-10.0	20.0
10.0-30.0	70.0
30.0-100.0	4.4

Figure 1. 5-minute time-series of plume height from the Icelandic radar (crosses), for the constant plume height simulation (solid), low plume height reconstruction (dashed) and high plume height reconstruction (doted). The grey area represents missing radar data due to missing scans (light grey) or clouds (dark grey). The minimum plume height detectable due to mountain ranges and curvature of the Earth is 2.5 km. Where no plume is detected (but radar data isn't missing), 2.5 km has been plotted.

diameter) present in the proximal ash deposits that range from 2% to 60% depending on the type of volcano. However, as discussed by *Mastin et al.* [2009] these estimates are based on a wide range of eruption types some of which generated pyroclastic density currents (producing large volumes of fine ash). As distal ash is often too widely dispersed to be sampled, even though collectively it is a significant mass, these estimates are frequently based on analysis of grain size distribution of deposits close to the volcano which may underestimate the fraction of distal fine ash [*Bonadonna and Houghton*, 2005]. In addition these measurements all refer to grain size and so will tend to overestimate the fraction of fine particles if there is significant aggregation. An estimation of the distal fine ash fraction for the initial phase of the eruption using a novel method based on modelled and remotely sensed observations of ash concentration is made in this paper.

2.4. Size Distribution Of Ash

All of the emitted mass in NAME is distributed among particles with a diameter drawn from the size distribution shown in table 1. This distribution is based on an average of measurements made in the plumes from explosive eruptions of Mount Redoubt on 8th January 1990, Mount St Helens on 18th May 1980 and St Augustine on 8th February 1976 [*Hobbs et al.*, 1991; *Leadbetter and Hort*, 2011]. Ash density in NAME is assumed to be 2300kg m^{-3}.

3. NAME Simulations

NAME is a Lagrangian particle trajectory model designed for many dispersion applications, including the prediction of the dispersion and deposition of volcanic ash in the atmosphere [*Jones et al.*, 2007]. Emission of volcanic ash is modelled by releasing ash particles into the model atmosphere (120,000 particles/hour for the simulations in this paper), with each model particle representing a mass of volcanic ash. The model ash particles are carried along by the wind with turbulent mixing represented by giving the trajectories a stochastic perturbation using semi-empirical turbulence profiles. NAME also includes treatments of sedimentation and dry and wet deposition [*Webster and Thomson*, 2008].

In this paper, NAME III (version 5.4) is driven using the 3D winds and thermodynamic fields from UK Met Office global NWP model analysis fields, updated every 6 hours and forecast fields updated every 3 hours. Ash concentrations are computed by summing the mass of ash particles in areas of 0.375° latitude by 0.5625° longitude (approximately 40 km×40 km), averaged over 200 m in the vertical and over a time period of 1 hour.

Plume height input is taken from measurements provided by the Icelandic Meteorological Office's C-band radar [*Petersen and Arason*, 2011] (http://andvari.vedur.is/ arason/radar/). Figure 1 shows the 5-minute time-series of plume height from the Icelandic radar. It is clear that the plume height from the radar varies on a range of timescales from minutes to hours. The grey shading represents missing radar data due to missing scans or clouds obscuring the ash plume. 89.4% of the data is missing between 09 UTC on 15 April and 03 UTC on 16 April. 46.3% due to missing scans, 36.6% due to cloud obscuring the ash plume and 6.5% due to plume height below 2.5km. The authors are not aware of any observations available to verify the plume height during this time. Therefore, in this paper three simulations of the Eyjafjallajökull volcano ash dispersion have been performed with different plume height input. For our control simulation a constant plume height of 8.5 km amsl was used for the first 96 hours of the simulation which began at 09 UTC on 14 April 2010. The second and third simulations used a varying plume height that represents the varying plume height detected by the radar in Iceland. Note that plume height variations are represented on timescales of 6 hrs or more. No attempt has been made to follow every fluctuation in the radar data. Values of plume height have been chosen to pass through the upper end of the scatter in the 5 minute radar values while not reflecting the most extreme values. For the period in which few radar observations were available, two reconstructions are made. In the first reconstruction the plume height is kept constant at 6 km from 09 UTC on 15 April until 03 UTC on 16 April at which point it is increased to 8.25 km, referred to in this paper as the low plume height reconstruction. In the second reconstruction the plume height is increased immediately from 6 km to 8.25 km amsl at 09 UTC on 15 April and then kept constant, referred to in this paper as the high plume height reconstruction. These reconstructions represent the uncertainty in the plume height input. For all three simulations ash was emitted uniformly between the volcano summit and the plume height.

4. Observations

From the 14-16 April 2010 a high-pressure system was located over the UK and the north Atlantic and a low-pressure system was located over northern Europe (figure 3(a)) resulting in the ash cloud being transported to the south-east. A decaying cold front associated with the low-pressure system was moving southwards over the UK. Mostly cloud-free skies over much of Europe during this period (figure 3(b)) allowed the ash cloud to be observed by several ground based lidars. Two such lidar retrievals were obtained at Chilbolton, in the south of England (51.1°N, 1.4°W), and at Leipzig in Germany (51.4°N, 12.4°E) on 16 April 2010.

4.1. Chilbolton lidar

Figure 2(a) shows the range-corrected lidar backscatter from the ground-based lidar at Chilbolton on 16 April 2010. The ash cloud was first observed over Chilbolton at a height of 3 km at 12 UTC on 16 April 2010. The height of the ash cloud decreased with time, and intercepted the boundary layer at 15 UTC. The *effective thickness* of the layer, defined as the total column mass divided by the peak mass concentration, was approximately 500 m. Figure 2(b) shows the ash mass concentrations derived by *Hogan et al.* [2011] from a combination of the ground-based lidar and sun-photometer measurements overlaid with the boundary layer top. The boundary layer top is estimated as the height at which the 1.5μm lidar backscatter signal is no longer significant (figure 2(a)). For the period during which the ash cloud intersects the top of the boundary layer, 15-15.30 UTC, the boundary layer height has been interpolated. The peak mass concentrations of $690 \pm 210\mu$g m^{-3} were retrieved at 14.34 UTC at a height of 1.7 km above the surface. Similar sloping ash plumes and concentrations were observed over Exeter on 16 April [*Marenco and Hogan*, 2010].
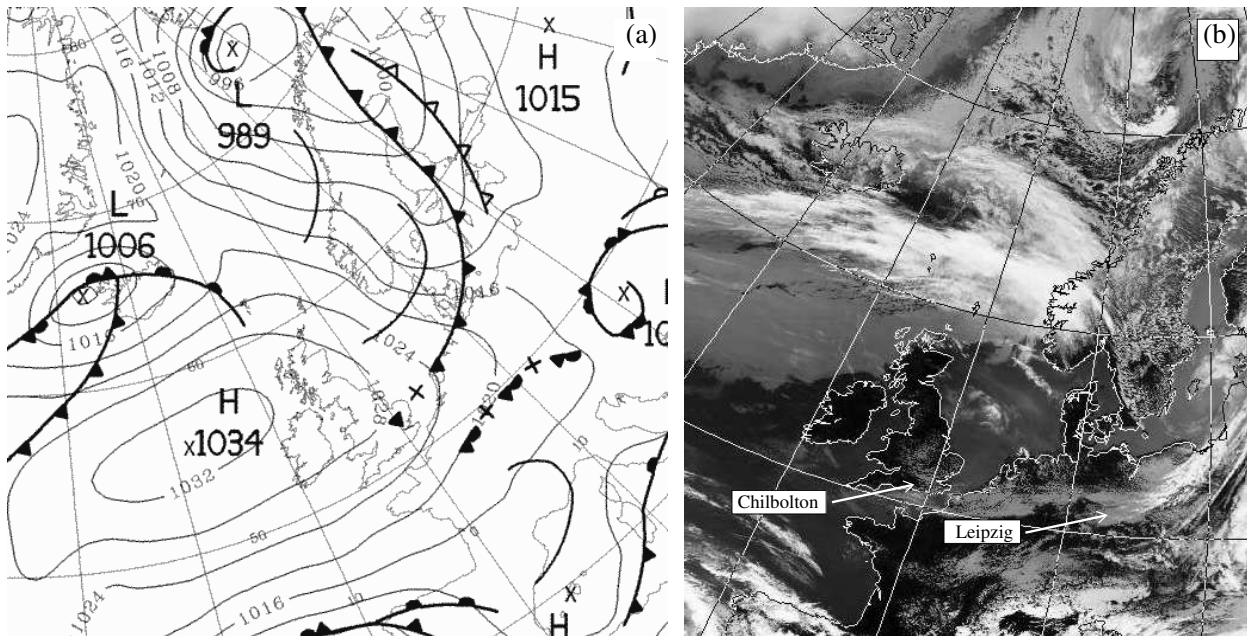
Figure 3. (a) Synoptic analysis at 00 UTC on 16 April 2010 from the UK Met Office. (b) AVHRR thermal infrared image $(11.5 - 12.5\mu m)$ at 12:55 UTC on 16 April 2010 courtesy of Dundee satellite receiving station.
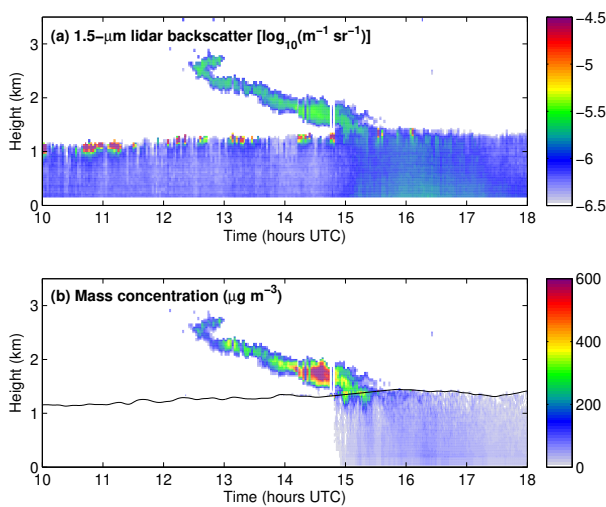

Figure 2. Time-height plots at Chilbolton $(51.1°N, 1.4°W)$ from 10-18 UTC on 16 April 2010. (a) lidar backscatter, and (b) mass concentration retrieved from a combination of lidar and sun photometer measurements overlaid with the boundary layer top (black line).

4.2. Leipzig lidar

Ansmann et al. [2010] also observed an ash cloud using the ground-based lidar at Leipzig on 16 April 2010 (*Ansmann et al.* [2010], their figure 1). The lidar observations at Leipzig were largely obscured by low-level cloud between 05 and 12 UTC on 16 April 2010 although ash was observed for a short time at 09:20 UTC, at a height of 5 to 7 km. From 12-18 UTC the base of the ash cloud decreased with time, as at Chilbolton, descending from 5-2 km. The ash cloud over Leipzig had an effective thickness of approximately 1 km

with peak mass concentrations of $1000\mu g$ m^{-3} retrieved between 12 and 13 UTC at a height of 3.2 km above the surface. The descent the ash cloud is not the result of a descending ash layer but is due to the advection of a sloping structure over Leipzig. This sloping structure was observed by NASA's Cloud-Aerosol Lidar and Infrared Pathfinder Satellite Observations (CALIPSO) satellite which captured an image of the volcanic ash cloud on 17 April as it drifted over Europe (http://atrain.nasa.gov/stories.php).

5. Constant plume height

In this section the NAME simulation of the initial phase of the eruption (14-16 April), using a constant plume height of 8.5 km amsl (control simulation), is summarised and compared with the observed ash cloud over Leipzig and Chilbolton.

5.1. Summary of initial phase of eruption

Figure 4 shows maps of column-integrated mass concentration obtained from the NAME control simulation for the initial phase of the eruption. It should be noted that the impression given in comparing observed and NAME-simulated ash concentration can be dependent on the contour interval chosen for plotting both the observed and modelled ash concentrations. In this paper NAME mass concentrations are plotted on a linear scale but an outline of the outermost extent of the simulated ash cloud is also plotted. The shaded part of the plume at 00 UTC on 15 April (figure 4(a)) contains 96% of the mass, the fraction reduces to 75% at 12 UTC on 16 April (figure 4(d)). An arbitrary scale is used to avoid implying quantitative predictions of ash concentrations at long-range where the distal fine ash fraction is not known.

Initially the NAME simulated ash cloud was advected south-eastwards from Iceland towards western Europe (figure 4(a)). After 24 hours the ash cloud began to diverge and transport occurred both northeastwards and southwestwards, parallel to the cold front associated with the low pressure system over Scandinavia (figure 3(a)). A branch of the ash cloud was advected over the UK (figure 4(b)) reaching Chilbolton $(51.1°N, 1.4°W)$ at 17 UTC on 15 April 2010 (figure 4(c)).
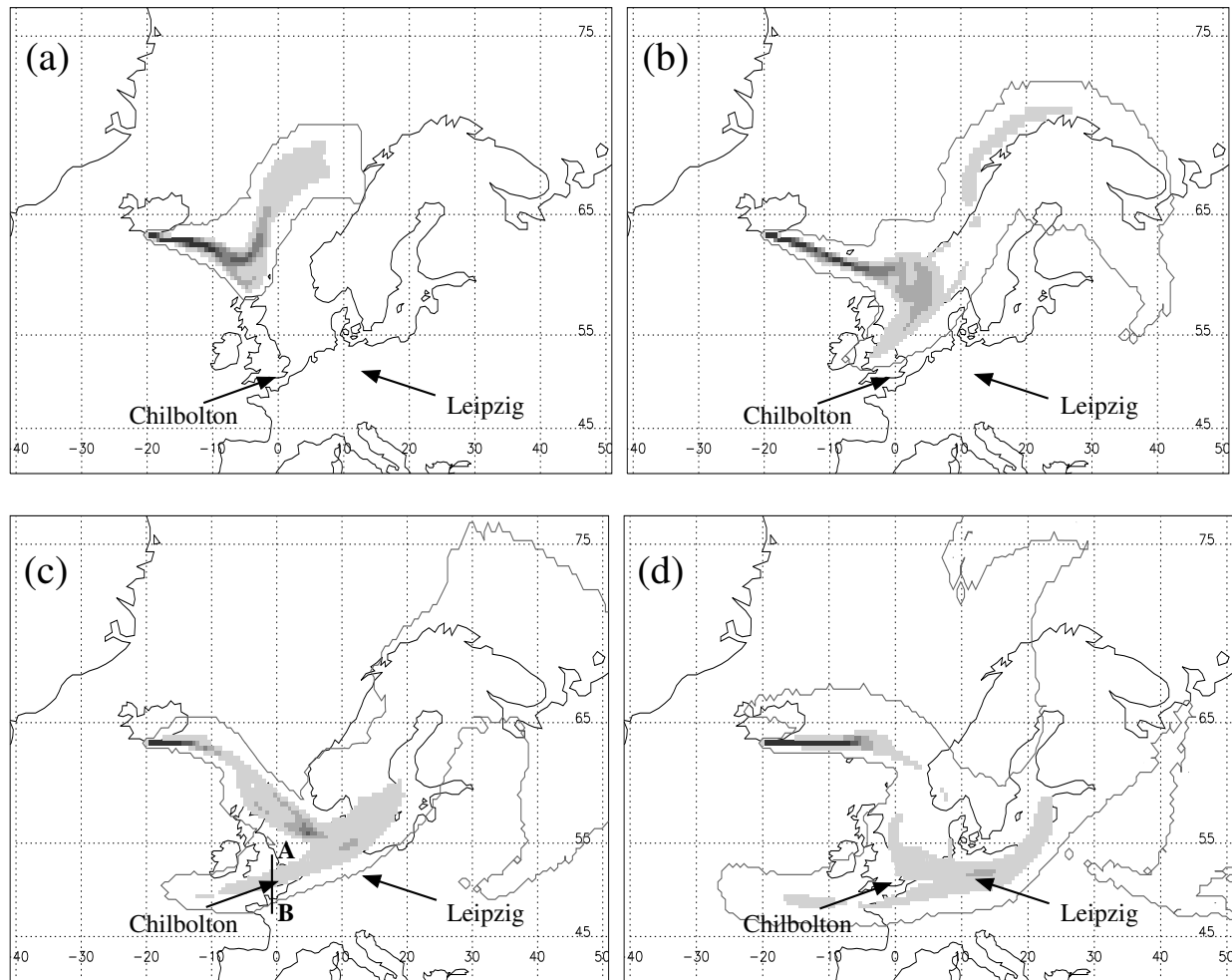
Figure 4. Column-integrated NAME mass concentration from the control simulation at (a) 00 UTC on 15 April 2010, (b) 12 UTC on 15 April 2010, (c) 00 UTC on 16 April 2010 and (d) 12 UTC on 16 April 2010. The shaded concentration contours are in arbitrary units, contours are equally spaced concentration levels and span a factor of 5 across the entire range of levels. The grey line outlines the outermost extent of the ash cloud. The black line, AB, indicates the location of the vertical cross-section in figure 5.

Figure 5 shows a vertical cross-section through the branch of the ash cloud that was forecast to be advected over the UK at 00 UTC on 16 April 2010 (along the line AB in figure 4(c)). The ash layer has a sloping structure that extends from 6 km to the surface. As with Leipzig, the descending base of the ash cloud observed over Chilbolton (figure 2) and the other UK lidars is the result of advection of a sloping structure over the sites and is not a result of a descending ash layer.

Table 2 shows the time at which volcanic ash was observed by ground-based lidars at Cardington, Reading, Chilbolton and Exeter in the UK (locations are shown in figure 6) as well as the time at which significant ash is present in the model at these locations. As the volcanic ash detection limit for each lidar is not known, it is not possible to set an equivalent threshold for ash concentrations in NAME. Therefore, in table 2, significant modelled ash concentration thresholds are defined as ash concentrations that are $> 1\%$ of the peak concentration predicted over each lidar location. The presence of significant ash concentrations over the 4 UK lidar lo-
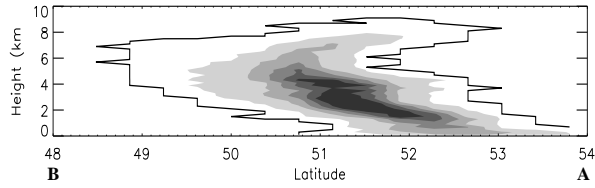
Figure 5. Vertical cross-section of mass concentration from 48°-54°N at 1.4°W (along line, AB, in figure 4(c)). The shaded concentration contours are in arbitrary units, contours are equally spaced concentration levels and span a factor of 5. The black contour outlines the outermost extent of the ash cloud.

cations in NAME has been determined for two layers of the atmosphere; between 1.2 and 12 km above the surface and between 1.2 and 3.2 km above the surface. The first layer encompasses the whole depth of the NAME simulated ash cloud as it passed over the UK and the second layer encompasses the depth of the atmosphere in which volcanic ash cloud was actually observed by the lidars in the UK. It is evident that a timing error exists between the NAME simulations and the observed ash at all of the UK lidar sites.

The NAME simulated ash travels southwards over the UK on the 15th and 16th April with a southwards velocity of ≈ 6 ms^{-1} in the west of the UK and ≈ 4 ms^{-1} in the east of the UK. The mean wind speed between 1.2 and 3.2 km measured by the 09 UTC 16 April radiosonde at Larkhill (51.2°N,1.8°W) was 9.7 ms^{-1} with a mean wind direction in the same layer of 51.8°, giving a southwards wind velocity of 6.0 ms^{-1}. This is consistent with the NAME simulated ash cloud propagation speed therefore the timing difference be-

tween the NAME simulation and the observed ash cloud over Chilbolton is unlikely to be due to an incorrect propagation speed. However, figure 6 shows the MODIS AQUA visible satellite image at 13:23 UTC on 16 April. An east-west orientated band of volcanic ash can be seen stretching from southern England to Belgium over the English Channel. The feature to the north is an algal bloom or sediment and can be distinguished from the ash cloud as it remains stationary whilst the ash cloud travels southwards. The location of this ash cloud corresponds well with the NAME simulated ash cloud at 00 UTC on 16 April (figure 4(c)). This suggests that the timing difference between the NAME simulation and the observed ash cloud over Chilbolton is caused by cumulative errors in the driving NWP wind fields used in NAME resulting in a positional error in the north-south direction of around 200 km.
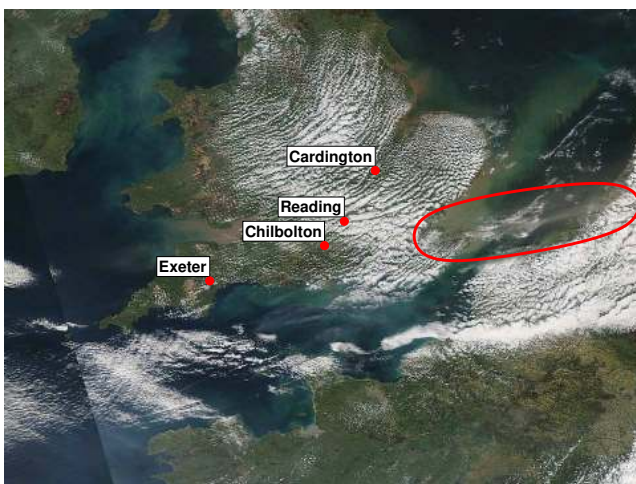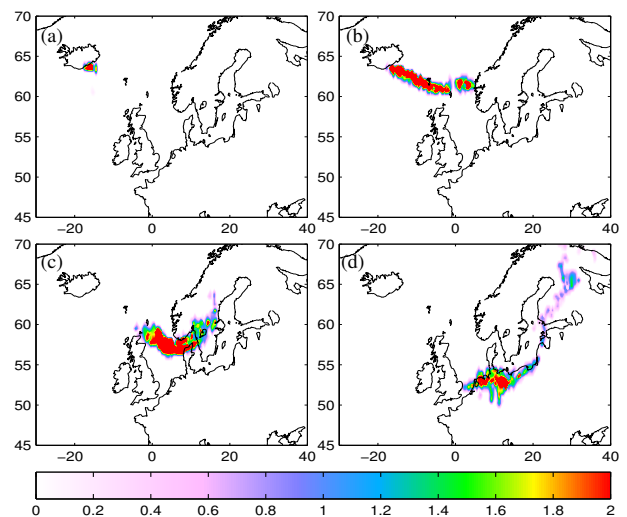

Figure 6. MODIS AQUA visible image at 13:23 UTC on 16 April showing a volcanic ash cloud (enclosed by the red contour) stretching from southern England to Belgium. The locations of the UK lidars at Cardington, Reading, Chilbolton and Exeter are overlaid.

Figure 7. IASI measured volcanic ash index (K) at (a) 22 UTC on 14 April 2010, (b) 10 UTC on 15 April 2010, (c) 22 UTC on 15 April 2010 and (d) 10 UTC on 16 April 2010.

Table 2. Volcanic ash over Cardington, Reading, Chilbolton and Exeter observed by ground-based lidars (crosses). NAME volcanic ash between 1.2 and 12 km (all circles) and between 1.2 and 3.2 km (filled circles only).

Location	Lat/Lon (°N,°W)		15/04/10									16/04/10																					
			15	16	17	18	19	20	21	22	23	00	01	02	03	04	05	06	07	08	09	10	11	12	13	14	15	16	17	18	19	20	21
Cardington	52.1,0.4	NAME	○	○	○	○	•	•	•	•	•	•	•	•	•	•	•																	
		Lidar																		×	×	×	×	×	×	×							
Reading	51.3,0.6	NAME			○	○	○	•	•	•	•	•	•	•	•	•	•	•															
		Lidar																						×	×	×							
Chilbolton	51.1,1.4	NAME				○	○	○	•	•	•	•	•	•	•	•	•	•	•	•	•												
		Lidar																					×	×	×	×	×						
Exeter	50.7,3.5	NAME	•	•	•	•	○	○	○	•	•	•	•	•	•	•	•	•															
		Lidar																						×	×	×	×	×	×	×	×	×	×

Figure 7 shows the ash cloud and its initial transport as measured by the Infrared Atmospheric Sounding Interferometer (IASI) on-board METOP-A. Infrared sounders are very sensitive to the presence of minerals [*Clarisse et al.*, 2010a]. Volcanic ash in particular has a very specific infrared signature [*Holasek and Rose*, 1991; *Schneider and Rose*, 1994; *Gangale et al.*, 2010], which makes it differentiable from other aerosols and clouds. The specific ash signature depends on the mineral composition and the particle size distribution of the ash and a general and robust method for detecting ash from high resolution infrared sounders was recently proposed in [*Clarisse et al.*, 2010b]. We have applied the method here on the first 4 IASI overpasses after the eruption and the result is shown in figure 7. Measurements have been quantified using an ash absorption index (brightness temperature difference between $1168cm^{-1}$ and $1231.5cm^{-1}$) for measurements which pass the ash detection test (and 0 for those that do not).

In the NAME simulation Leipzig is close to the central axis of the ash cloud and ash was transported over Leipzig at 05 UTC on 16 April (figure 4(d)). Figure 7 shows the ash measured by IASI. The ash cloud does not show up in it's entirety due to the detection limits of the instrument and the presence of cloud. However, the spatial correlation of the IASI ash cloud and the highest concentrations in the main part of the NAME cloud (figures 4(a)-(d)) is remarkably good. Particularly over Leipzig (figures 4(d) and 7(d)) suggesting that NAME correctly predicts the time of arrival of the ash cloud at the central axis over Leipzig.
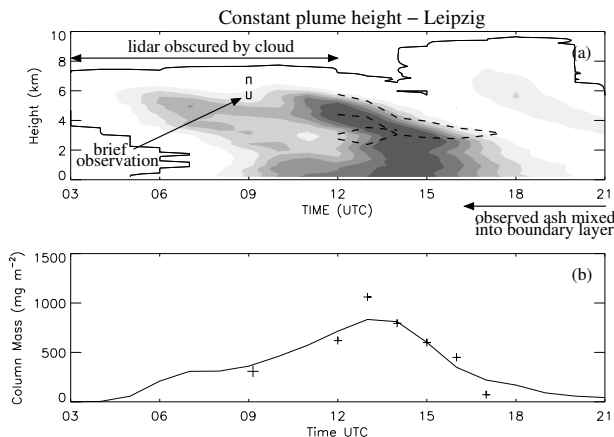
Figure 8. Constant plume height simulation on 16 April 2010. (a) Time-height plot of NAME mass concentration over Leipzig (51.4°N, 12.4°E) on 16 April 2010 overlaid with the outline of the lidar ash cloud (dashed). The shaded concentration contours are in arbitrary units, contours are equally spaced concentration levels and span a factor of 6. The solid black contour outlines the outermost extent of the modelled ash cloud. (b) Time-series of above boundary layer integrated mass loading over Leipzig, from NAME (solid) and the lidar retrieval (crosses).

5.2. Constant plume height - Leipzig

Figure 8(a) shows NAME mass concentration results for Leipzig with the outline of the lidar ash cloud overlaid. Note that the lidar observations at Leipzig were largely obscured by low-level cloud between 05 and 12 UTC on 16 April 2010. Ash was briefly detected at 09 UTC in a layer between 5 and 7 km. NAME shows significant amounts of ash arriving over Leipzig at 05 UTC, with the top of the ash cloud at 6 km, and maximum mass concentrations centred at 5 km. Between 12 and 15 UTC NAME captures the sloping upper ash layer seen by the lidar although in NAME the layer appears to be about 500 m lower than the observed layer and towards the end of this period, the NAME ash cloud extends to the ground. Mixing of ash into the boundary layer is also observed by *Ansmann et al.* [2010] after 16 UTC. The ash layer centred at 3 km seen in the lidar observations after 12 UTC is not apparent in NAME but NAME shows an increase in ash concentration below 3 km.

Figure 8(b) compares time series of the column-integrated mass loading derived from NAME and the Leipzig lidar measurements. The lidar mass loadings have been calculated by integrating from the top of the boundary layer upwards as the *Ansmann et al.* [2010] measurements include backscatter from boundary layer aerosol while the NAME mass loadings are calculated by integrating from 1.2 km upwards. The quantitative agreement between NAME and the lidar observations is obtained by assuming that the distal fine ash fraction is 1.5%, i.e. the NAME mass concentrations match the observed concentrations if the modelled concentrations are scaled by 1.5%. This suggests that 98.5% of the emitted mass falls out close to the source. There are of course uncertainties in this figure arising from inaccuracies in the modelling (including any inaccuracies in the mass emission rate). The distal fine ash fraction is assumed to be constant with time.

5.3. Constant plume height - Chilbolton

Figure 9(a) shows the NAME results for Chilbolton with the outline of the lidar ash cloud overlaid. The NAME simulation shows a layer of ash with a sloping structure extending between 6 km and 1 km. A hook like feature is also seen in the NAME simulation from 6 km to 8 km bending back over the top of the sloping structure. As discussed in section 5.1, in NAME the ash cloud arrives earlier than was observed over Chilbolton. Therefore, for this comparison, the NAME ash cloud has been shifted into the future by 9 hours so that the sloped structure of the NAME ash cloud and the observed ash cloud coincide. A shift of 9 hours is assumed for the Chilbolton ash cloud for the remainder of this paper. This shift is consistent with the observations from other UK lidars in Exeter, Cardington and Reading (see table 2). Between 13 and 17 UTC
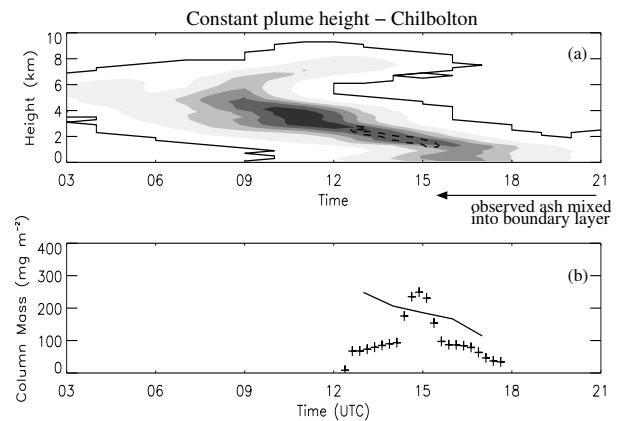

Figure 9. Constant plume height simulation on 16 April 2010. (a) Time-height plot of mass concentration over Chilbolton (51.1°N, 1.4°W) on 16 April 2010 overlaid with the outline of the lidar ash cloud (dashed). The NAME results have been shifted by 9 hours so that the vertical structure of the NAME ash cloud and the observed ash cloud coincide. The shaded concentration contours are in arbitrary units, contours are equally spaced concentration levels and span a factor of 5. The solid black contour outlines the outermost extent of the modelled ash cloud. (b) Time-series of above boundary layer integrated mass loading over Chilbolton, from NAME (solid) and the lidar retrieval (crosses). NAME column-integrated mass loading are only plotted for the time during which the NAME and lidar observations match.

NAME captures the sloped ash layer seen by the lidar, although the NAME layer has an effective thickness of approximately 2 km compared to an observed ash cloud effective thickness of 500 m. Earlier NAME shows significant amounts of ash arriving at Chilbolton between 4 and 8 km which was not observed by any of the 4 UK lidars that detected ash. Potential causes of this difference are discussed in section 6.

Figure 9(b) shows estimates of the column integrated ash derived from the Chilbolton lidar measurements [*Hogan et al.*, 2011] compared with those calculated from NAME for the period during which the NAME and lidar observations match, i.e. between 13 and 17 UTC only. The lidar and NAME mass loadings have been calculated by integrating from the surface. The quantitative agreement between NAME and the lidar observations is obtained by assuming a distal fine ash fraction of 2%. This is a similar scaling used to gain quantitative agreement between the NAME simulations and the Leipzig lidar and for the lidar at Exeter [*Marenco and Hogan*, 2010; *Devenish et al.*, 2011]. Thus it appears that using a constant plume height NAME is able to capture the structure and timing of the ash cloud over Leipzig but, although the sloped structure of the ash cloud is captured over Chilbolton, the upper-level ash and the timing of the ash cloud does not agree with the UK lidar observations.

6. Varying plume height

In this section we investigate the potential causes of the NAME over-prediction of ash between 4 and 8 km over Chilbolton. One potential explanation is missing processes in NAME such as aggregation and electrostatic charging of ash particles. During the initial phreatomagmatic phase of the eruption, significant cirrus cloud was generated. Ice crystal growth on ash particles followed by turbulence-induced aggregation, wet aggregation (as the ash-hydrometeors pass through the melting level [*Durant et al.*, 2009]), and increased electrostatic binding of ash-hydrometeors [*James et al.*, 2002; *Harrison et al.*, 2010] results in rapid aggregate fallout due to increased sedimentation. Thus aggregation processes significantly reduce the proximal fine ash fraction and alter the effective particle size distribution. Although aggregation is most effective near the source, aggregation of small grains can also occur > 1000 km from the source, due to the interaction of ash and ice particles. Aggregation processes occurring in the distal ash cloud are not represented in NAME. However, *Rose et al.* [2000] and *Folch et al.* [2010] show that the effect of aggregation in the distal ash cloud is likely to be small. Thus, it is unlikely that missing aggregation processes in the distal ash cloud can explain the over-prediction of ash between 4 and 8 km over Chilbolton.

Another potential cause of the NAME over-prediction of ash between 4 and 8 km over Chilbolton could be that errors in the driving wind fields led to upper-level ash being transported in the wrong direction particularly at the complex divergence point on the cold front. In this case, the upper-level ash transported over Chilbolton in NAME would have been transported over mainland Europe instead. However, the CALIPSO satellite image on 17 April taken over mainland Europe does not show ash higher than 5.5 km amsl.

Other potential causes of the NAME over-prediction of ash between 4 and 8 km over Chilbolton are the failure in our control simulation to represent the variations in plume height that were observed in the early phase of the eruption (figure 1) and the potential difference between the maximum observed plume height and the maximum height at which ash was injected laterally into the atmosphere. It is quite likely that a constant plume height of 8.5 km, used in the NAME simulation in section 5, overestimates the actual plume height at the time at which ash contributing to the Chilbolton ash cloud was emitted.

Simulations have been performed in which a time varying plume height was used to determine the impact of variations in plume height on long range volcanic ash predictions. The plume height estimates have been obtained from the Icelandic radar. Where radar observations are mostly missing (09 UTC on 15 April to 03 UTC on 16 April) two reconstructions have been made. In the first reconstruction the plume height was kept constant at 6 km (low plume height reconstruc-
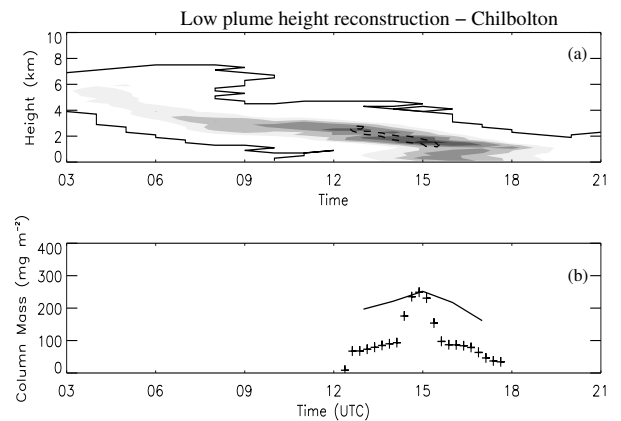

Figure 10. As figure 9 but for low plume height reconstruction simulation over Chilbolton.

tion). In the second reconstruction the plume height was kept constant at 8.25 km (high plume height reconstruction).

6.1. Low plume height reconstruction - Chilbolton

Figure 10(a) shows the mass concentration over Chilbolton for the low plume height reconstruction simulation. Varying the plume height affects both the maximum ash cloud depth and the mass concentrations of the simulated ash cloud over Chilbolton. Compared to the constant plume height simulation (figure 9(a)) the maximum ash cloud depth has decreased by 3 km. The vertical distribution of ash now agrees better with the Chilbolton lidar observations. The magnitude of the mass concentrations also reduces as the plume height reduces (due to equation (1), in the Appendix). In order to agree with the estimated column loadings from the lidar observations (figure 10(b)) the distal fine ash fraction has been increased from 2% to 3%.
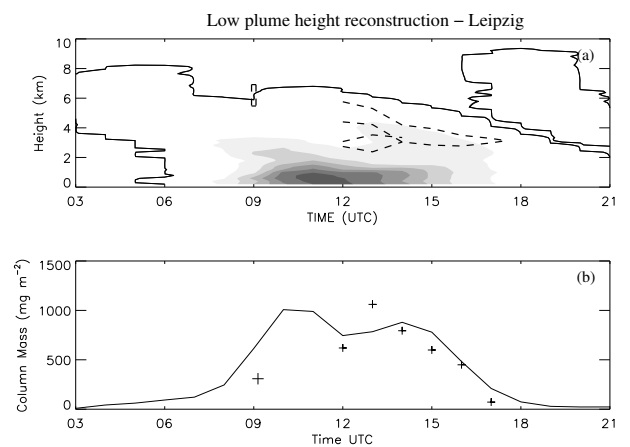

Figure 11. As figure 8 but for low plume height reconstruction simulation over Leipzig.

6.2. Low plume height reconstruction - Leipzig

Figure 11(a) shows the NAME ash cloud at Leipzig for the low plume height reconstruction simulation. The upper-layer of ash observed in the lidar observations after 12 UTC on 16 April and the early arrival of the ash cloud between 5 and 7 km at 09 UTC are now not predicted by NAME. Thus using the low plume height reconstruction produces a prediction that does not agree as well as the constant plume height prediction over Leipzig. In addition, the distal fine ash fraction estimated from the column loadings (figure 11(b)) would need to be increased from 1.5% to 10%.

Thus the NAME simulation and the Leipzig lidar observations are more consistent when emission is spread throughout the column over a range of heights up to 8.5 km amsl.

6.3. Mean emission time

In order to determine whether or not ash emitted at the same time contributed to the ash observed at both Chilbolton and Leipzig the mean emission time of the material contributing to each concentration estimate has been estimated (for the constant plume height case). The *mean emission time* is defined as the mean time at which ash particles contributing to the concentration in a volume of the atmosphere are emitted from the volcano. In these NAME simulations the volume of the atmosphere is approximately 40 km×40 km in the horizontal and 200 m in the vertical. Note that the mean emission time will not be a good representation if the minimum and maximum emission times in the (space-time) averaging volume are significantly different. However, the high vertical resolution of the NAME simulations (200 m) and high temporal resolution (hourly) means that this uncertainty should be small. Figure 12(a) shows the mean emission time for ash particles over Chilbolton in the constant plume height simulation. It is assumed that although the NAME ash cloud arrives over Chilbolton 9 hours earlier than observed, due to a small error in the position
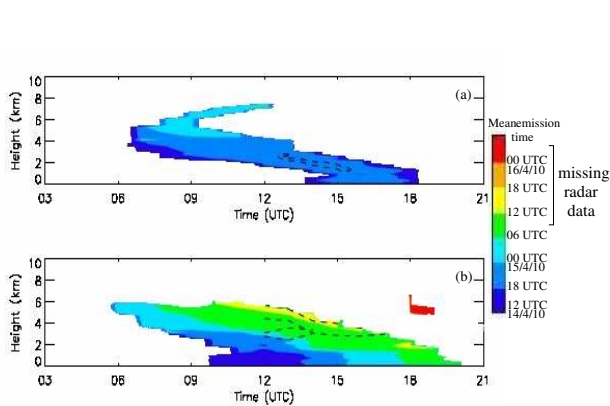
of the ash cloud moving southwards over the UK, the time of the emission in the model is appropriate without any correction. Figure 12(a) shows that the upper-part of the NAME ash cloud over Chilbolton was emitted, on average, between 00 and 06 UTC on 15 April. The sloping part of the ash cloud, which corresponds to the observations, was emitted earlier, on average between 18 UTC on 14 April and 00 UTC on 15 April. Thus if the plume height was overestimated between 00 and 06 UTC on 15 April as suggested by the Icelandic Meteorological Office radar measurements (fig 1) this could have led to an overestimation of the ash cloud height at Chilbolton.

Figure 12(b) shows the mean emission time for the constant plume height NAME simulated ash particles over Leipzig. Ash emitted in separate 6-hour intervals extends in coherent sloped layers from 6 km down to 1 km. It is interesting that what appears as a single ash cloud over Leipzig actually has complex structure when viewed in this manner. As for Chilbolton, ash near the surface was released at an earlier time than ash aloft. Comparison of the Chilbolton and Leipzig emission times shows that the ash emitted after 06 UTC on 15 April contributes to Leipzig but not to Chilbolton. Thus it is hypothesized that after 09 UTC on 15 April, during the period for which there were few radar observations, the plume height increased significantly from the 6 km value estimated to apply before 09 UTC to something closer to the 8.5 km value used in section 5.

6.4. High plume height reconstruction

Figure 13(a) shows the mass concentration over Leipzig for the high plume height reconstruction simulation. The upper-layer of ash is captured by the NAME simulation as well as the early arrival of the ash cloud at 09 UTC. For quantitative agreement with the lidar column loadings the distal fine ash fraction is 4%. The comparison between NAME and Chilbolton lidar (not shown) is very similar to figure 10(a), as both the
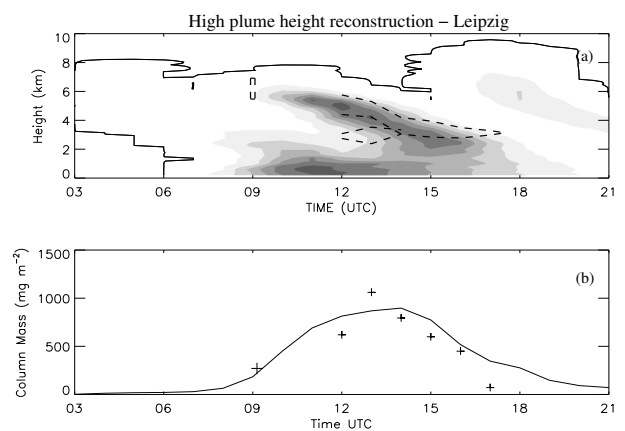

Figure 12. Time-height plots of mean emission time on 16 April 2010 at (a) Chilbolton and (b) Leipzig for the constant plume height simulation.

Figure 13. As figure 8 but for high plume height reconstruction simulation over Leipzig.

low and high plume height reconstructions have plume height ≤ 6 km between 00 and 09 UTC on 15 April compared to the constant plume height of 8.5 km.

7. Discussion and Conclusions

The Eyjafjallajökull volcano in Iceland started to emit high concentrations of ash into the atmosphere on 14 April 2010. Ash emitted by the volcano was transported towards Europe and was observed by lidars at Reading, Cardington, Exeter and Chilbolton in England, and Leipzig in Germany on 16 April 2010. The UK Met Office dispersion model (NAME) has been used to simulate the evolution of the volcanic ash cloud and results have been compared to lidar observations. Leipzig was close to the central axis of the ash cloud, while the UK lidars were to the west of it. The transport of ash over the UK appears to have been parallel to a front associated with a low-pressure system centered to the north of Scandinavia.

The accuracy of the NAME simulations depends on the accuracy of driving meteorological fields and volcano source parameters such as the plume height. The Icelandic radar observational data, used as plume height input, is mostly missing for an 18 hour period during the initial phase of the eruption. In this paper NAME simulations have been compared to lidar observations made at Chilbolton and Leipzig using 3 different plume height input reconstructions.

Taken together the Leipzig and Chilbolton observations are consistent with NAME if the volcanic plume height input represents the large variations on timescales of order 6 hrs in the plume height. These variations are broadly consistent with the Icelandic radar data. As a word of caution, using Chilbolton (or all of the UK lidars) only to perform the comparison would have given an incorrect or ambiguous estimation of plume height. Model and observation comparisons are needed over a wide area, encompassing different parts of the ash cloud in order to give a low variance reconstruction. These results highlight the danger of using single observations to assess the performance of models in complex meteorological situations. They also show that it is necessary to accurately represent variations in emission height to produce accurate predictions. Therefore it matters how we cope with missing data, even for short periods.

Overall, NAME appears to capture both the timing and vertical structure of the ash near the central axis of the ash cloud. Relatively small errors in the plume position, probably caused by the cumulative effect of errors in the driving meteorology en route, result in an timing error at distances far from the central axis of the ash cloud. Taking the timing error into account, NAME is able to capture the sloped ash layer over the UK. Quantitative comparison with the observed mass concentrations at Chilbolton and Leipzig suggests that

around 3% of the total emitted mass is transported over long distances by small ($< 100\mu m$ diameter) ash particles.

Further work is desirable to investigate the meteorological timing error using ensemble meteorological analysis fields. Further work is also needed for later periods of the eruption to constrain further estimates of the distal fine ash fraction and to determine the sensitivity of this number to the assumed particle size distribution and the vertical distribution of ash at the source. A detailed study of the near field plume behaviour, particularly for weak plumes involving strong interactions with the background atmosphere, would be beneficial for future volcanic eruptions.

Appendix: Mass Eruption Rate

In this paper the relationship relating the observed maximum plume height to the eruption rate is given by;

$$H = 0.365M^{0.225}, \qquad (1)$$

where H (km) is plume height above volcano summit and M (kg/s) represents the total mass eruption rate. The power law in this empirical relationship is based on a fit to a look-up table constructed by the National Oceanic and Atmospheric Administration (NOAA) for the VAFTAD (Volcanic Ash Forecast Transport and Dispersion) model and reproduced in *Leadbetter and Hort* [2011]. The table gives threshold model concentrations to be used with a model releasing a nominal 1g/6hr in order to determine the extent of visual ash. This threshold depends on both summit height and plume height but here we have restricted consideration to a summit height equal to that of Eyjafjallajökull. Interpreting the threshold as inversely proportional to the actual emission rate means that the table can be inter-
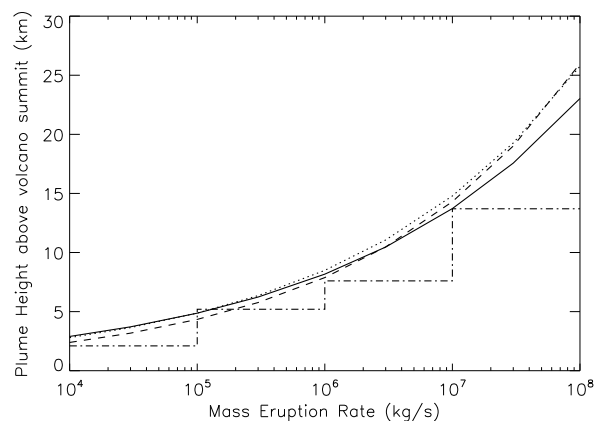

Figure 14. The variation of eruption rate with plume height used in NAME, $H = 0.365M^{0.225}$ (solid), Mastin et al. (2009), $H = 0.304M^{0.241}$ (dotted), Sparks et al. (1997), $H = 0.220M^{0.259}$ (dashed) and the emission rates from the NOAA VAFTAD thresholds (dash-dot).

preted as giving the shape of the M(H) function. The table gives a step function with changes in threshold (or source strength) in factors of 10 but a smooth power law was fitted through the data. The pre-factor was then determined by comparing the values to the best fit curve given by *Mastin et al.* [2009]. Both in fitting the power law and determining the prefactor, the VAFTAD step function was regarded as most reliable at the top of each plume height range, and so only these values were used. This is based on the assumption that it was designed to ensure safety, and safety at the top of each height range implies that the safety margin at the bottom of each height range is larger than necessary. Figure 14(a) shows how equation (1) relates to the empirical relationships of *Mastin et al.* [2009] and *Sparks et al.* [1997] and the emission rates estimated from the NOAA VAFTAD thresholds. The VAFTAD table was used by the London VAAC up until the eruption of Eyjafjallajökull and is used by the Washington VAAC. Equation (1) was developed by the London VAAC during the eruption of Eyjafjallajökull.

References

Ansmann, A., M. Tesche, S. Grob, V. Freudenthaler, P. Seifert, A. Hiebsch, j. Schmidt, U. Wandinger, I. Mattis, D. Muller and M. Wiegner (2010), The 16 April 2010 major volcanic ash plume over central Europe: EARLINET lidar and AERONET photometer observations at Leipzig an Munich, Germany. *Geophys. Res. Letters.*, *37*, doi:10.1029/2010GL043809.

Bonadonna, C., G. Macedonio and R. Sparks (2002). Numerical modelling of tephra fallout associated with dome collapses and Vulcanian explosions: application to hazard assessment on Montserrat, in The Eruption of Soufrire Hills Volcano, Montserrat, From 1995 to 1999, edited by T. Druitt and B. Kokelaar, pp. 517-537, *Geol. Soc., London.*

Bonadonna, C., and B. F. Houghton (2005). Total grain-size distribution and volume of tephra-fall deposits, *Bull Volcanol*, *67*, doi 10.1007/s00445-004-0386-2

Casadevall, T. J. (1994). The 1989-1990 eruption of Redoubt volcano, Alaska: impacts on aircraft operations. *Journal of volcanology and geothermal research*, *62*, 301-316.

Clarisse, L., D. Hurtmans, A. J. Prata, F. Karagulian, C. Clerbaux, M. D.-Maziere and P.-F. Coheur (2010). Retrieving radius, concentration, optical depth, and mass of different types of aerosols from high-resolution infrared nadir spectra. *Applied Optics*, *49*, 3713-3722, doi:10.1364/AO.49.003713

Clarisse, L., F. Prata, J.-L. Lacour, D. Hurtmans, C. Clerbaux, and P.-F. Coheur (2010). A correlation method for volcanic ash detection using hyperspectral infrared measurements, *Geophys. Res. Lett.*, *37*, L19806, doi:10.1029/2010GL044828.

Devenish, B. J., D. J. Thomson, F. Marenco, S. J. Leadbetter and H. Ricketts (2011), A study of the arrival over the United Kingdom in April 2010 of the Eyjafjallajökull ash cloud using ground-based lidar and numerical simulations. *Submitted to Atmos. Env.*

Dubovik, O. and M. K. King (2000), A flexible inversion algorithm for retrieval of aerosol optical properties from Sun and sky radiance measurements. *J. Geophys. Res.*, *105*, 20673-20696.

Durant, A. J., W. I. Rose, A. M. Sarna-Wojcicki, S. Carey, and A. C. M. Volentik (2009), Hydrometeor-enhanced tephra sedimentation: Constraints from the 18 May 1980 eruption of Mount St. Helens, *J. Geophys. Res.*, *114*, B03204, doi:10.1029/2008JB005756.

Folch, A., A. Costa, A. Durant and G. Macedonio (2010). A Model for Wet Aggregation of Ash Particles in Volcanic Plumes and Clouds: II. Model Application, *J. Geophys. Res.*, *115*, B09202.

Gangale, G., A.J. Prata, L. Clarisse (2010). The infrared spectral signature of volcanic ash determined from high-spectral resolution satellite measurements, *Remote Sensing of Environment*, *114*, 414-425, DOI: 10.1016/j.rse.2009.09.007.

Guffanti, M., G. C. Maybery, T. J. Casadevall and R. Wunderman (2009). Volcanic hazards to airports. *Natural Hazards*, *51*, 287-302.

Guffanti, M., T. J. Casadevall, K. Budding (2010). Encounters of aircraft with volcanic ash clouds; A compilation of known incidents, 1953-2009: U.S. Geological Survey Data Series 545, ver. 1.0, 12 p., plus 4 appendixes including the compilation database, available at http://pubs.usgs.gov/ds/545

Harrison, R. G., K. A. Nicoll, Z. Ulanowski and T. A. Mather (2010). Self-charging of the Eyjafjallajökull volcanic ash plume. *Environmental Research Letters.* 5 024004 doi: 10.1088/1748-9326/5/2/024004.

Heffter, J. L., and B. J. B. Stunder (1993), Volcanic Ash Forecast Transport And Dispersion (VAFTAD) Model. *Wea Forecasting*, *8*, 534-541.

Hobbs, P. V., L. F. Radke, J. H. Lyons, R. J. Ferek, D. J. Coffman (1991). Airborne measurements of particle and gas emissions from the 1990 volcanic eruptions of Mount Redoubt. *J. Geophys. Res.*, *96*, 18735-18752.

Hogan, R. J., J. M. Haywood, H. F. Dacre, C. D. Westbrook, E. J. O'Connor, F. Marenco, C. L. Wrench and S. E. Belcher (2011). Lidar and sun-photometer retrievals of ash particle size and mass concentration from the Eyjafjallajökull volcano. *To be submitted to J. Geophys. Res..*

Holasek, R. E., and W. I. Rose. (1991), Anatomy of 1986 Augustine volcano eruptions as recorded by multispectral image processing of digital AVHRR weather satellite data. *Bull. Volcanol.*, *53*, 420-435

James, M. R., and J. S. Gilbert, and S. J. Lane (2002), Experimental investigation of volcanic particle aggregation in the absence of a liquid phase, *J. Geophys. Res*, *107*, doi:10.1029/2001JB000950

Jones, A., D. Thomson, M. Hort and B. Devenish (2007), The UK Met Office's next-generation atmospheric dispersion model, NAME III. Air pollution modeling and its application XVII. Edited by C. Borrego and A-L. Norman.

Leadbetter, S. J. and M. C. Hort (2011). Volcanic ash hazard climatology for an eruption of Hekla Volcano, Iceland. *J. Volcanol. Geotherm. Res.*, *199*, 230-241.

Marenco, F., and R. J. Hogan (2010). Determining the contribution of volcanic ash and boundary layer aerosol in backscatter lidar returns: a three-component atmosphere approach. *Submitted to J. Geophys. Res..*

Mastin, L. G., M. Guffanti, R. Servrancks, P. Webley, S. Barsotti, K. Dean, A. Durnat, J. W. Ewert, A. Neri, W. I. Rose, D. Schneider, L. Siebert, B,. Stunder, G. Swanson, A. Tupper, A. Volentik and C. F. Waythomas (2009). A multidisciplinary effort to assign realistic source parameters to moels of volcanic ash-cloud transport and dispersion during eruptions. *J. of Volcanol. Geotherm. Res.. 186.* 10-21.

Petersen, G. N. and P. Arason (2011). Radar observations of the altitude of the volcanic plume during the eruption of Eyjafjallajökull, April-May 2010. *Submitted to J. Geophys. Res.*

Rose, W. I., G. J. S. Bluth and G. G. J. Ernst (2000). ntegrating Retrievals of Volcanic Cloud Characteristics from Satellite Remote Sensors: A Summary. *Philosophical Transactions*, *358*. 1585-1606.

Schneider, D. J., and W. I. Rose (1994), Observations of the 1989-90 Redoubt Volcano eruption clouds using AVHRR satellite imagery, *U.S. Geol. Surv. Bull.*, *2047*, 405-418

Sparks, R. S. J., M. Bursik, S. N. Carey, J. A. Gilbert, L. S. Glaze, H. Sigurdsson and A. W. Woods (1997). *Volcanic Plumes.* John Wiley and Sons. Chichester.

Webley, P.W., Stunder, B.J.B., and K.G. Dean (2009), Significant eruption source parameter(s) for operational ash cloud transport and dispersion models.*Journal of Volcanology and Geothermal Research, 186,* 108 - 119.

Webster, H. N., and D. J. Thomson (2008). Dry deposition modelling in a Lagrangian dispersion model. *Proceedings from the 12th Harmonisation conference*, Cavtat, Croatia, 6-9 October 2008.

Wilson, L., R. Sparks, T. Huang, and N. Watkins (1978). The control of volcanic column heights by eruption energetics and dynamics *J. Geophys. Res., 83,* 1829-1836.

Witham, C. S., M. C. Hort, R. Potts, R. Sevranckx, P. Husson and F. Bonnardot (2007). Comparison of VAAC atmospheric dispersion models using the 1 November 2004 Grimsvotn eruption. *Meteorological Applications, 14,* 27-38.